



# Severe Autoimmune Thyroiditis in Transgenic NOD.H2<sup>h4</sup> Mice Expressing Interleukin-4 in the Thyroid

Karima Merakchi, Sami Djerbib, Jacques-Emile Dumont, Françoise Miot, and Xavier De Deken

**Background:** Hashimoto's thyroiditis is a common autoimmune thyroid disorder characterized by thyroid lymphocytic infiltrates and autoreactive antibodies against thyroglobulin (TgAbs) and thyroperoxidase. Final evolution of the disease can lead to hypothyroidism with destruction of the thyroid architecture. Interleukin-4 (IL-4) is involved in the humoral immune response and B cell activation required in autoimmune thyroiditis (AT) progression. We used our mouse model overexpressing IL-4 by thyrocytes (Thyr-IL4) to study the impact of a local IL-4 expression in AT using transgenic nonobese diabetic (NOD.H2<sup>h4</sup>) derived animals treated with iodide-supplemented water to increase the incidence of spontaneous AT (SAT).

**Methods:** Thyr-IL4 NOD.H2<sup>h4</sup> and nonpathogenic C57BL/6 animals aged 8 weeks were exposed to 0.05% sodium iodide (NaI) in their drinking water for 8 and 16 weeks. Circulating TgAbs and expression of intrathyroidal cytokines were quantified. Thyroid inflammation was assessed by classical histological analyses, including identification of some immune cell populations. The most sensitive parameter to evaluate the thyroid function, serum thyrotropin (TSH), was also measured at the end of the treatment.

**Results:** Relative to wild-type (WT) animals, Thyr-IL4 NOD.H2<sup>h4</sup> mice developed severe accelerated SAT with elevated serum TgAbs and numerous thyroid infiltrates mainly composed of CD4<sup>+</sup>/CD8<sup>+</sup> T cells, B lymphocytes, and monocytes/macrophages. Thyroid expression of T helper (Th) Th1/Th2 cytokines was also enhanced, as well as IL-17. In contrast, excessive iodide supply did not induce TgAbs in WT and Thyr-IL4 SAT-resistant C57BL/6 animals. However, moderate leukocyte infiltrations in transgenic thyroids were evident compared to WT, but associated with a limited number of T and B cells and a different cytokine profile from Thyr-IL4 NOD.H2<sup>h4</sup> mice. Finally, and despite their diverse immune responses, both transgenic strains presented marked thyroid enlargement and elevated serum TSH at the end of the treatment in contrast to their WT littermates.

**Conclusions:** These findings demonstrated that ectopic expression of IL-4 from thyrocytes enhanced the severity of accelerated SAT in disease-prone Thyr-IL4 NOD.H2<sup>h4</sup> animals and promoted thyroid leukocyte infiltration in SAT-resistant transgenic C57BL/6 mice. Moreover, impaired thyroid function emerged in both transgenic strains during the progression of the disease.

**Keywords:** autoimmunity, IL-4, thyroid, thyroiditis, transgenic mice

## Introduction

IODINE IS ESSENTIAL for the synthesis of triiodothyronine/thyroxine (T3/T4) thyroid hormones (TH) and is actively transported by thyroid follicular cells (TFCs) through the basal Na<sup>+</sup>/I<sup>-</sup> symporter NIS.<sup>1</sup> In susceptible individuals, iodine overload can cause autoimmune thyroiditis (AT).<sup>2</sup> Increased incidence of AT was clearly reported in multiple countries with iodized salt supplementation programs to correct iodine defi-

ciency.<sup>3</sup> Hashimoto's thyroiditis is the most frequent organ-specific autoimmune disease affecting mostly the female population.<sup>4</sup> This autoimmune disorder is characterized by thyroid lymphocytic infiltrates and circulating autoantibodies against the main thyroid antigens thyroperoxydase (TPO) and thyroglobulin (TG).<sup>5</sup>

Different mouse models have been developed to study the etiology of this human disease (reviewed in Quarantino<sup>6</sup>). Experimental AT (EAT) can be induced in C57BL/6 mice

after immunization with recombinant mouse Tpo.<sup>7</sup> Despite a clear destruction of TFCs in immunized mice, serum T4 levels remain normal. In contrast to C57BL/6, nonobese diabetic (NOD.H2<sup>h4</sup>) mice develop spontaneous AT (SAT), which is accelerated after iodized water supplementation. Excessive iodination of Tg facilitates the generation of new pathogenic epitopes and is believed to promote SAT in NOD.H2<sup>h4</sup> animals.<sup>8</sup> The SAT severity is well correlated with serum titers of autoantibodies against murine Tg (mTg; antibodies against thyroglobulin [TgAbs]).<sup>9,10</sup> While almost 100% of the mice develop thyroid lesions, serum T4 levels are again not significantly altered by the excessive iodide ingestion.<sup>11,12</sup>

Increased serum levels of the T helper (Th) Th1 cytokine IFN $\gamma$  with accumulation of peripheral Th1 cells are frequently observed in patients suffering of severe Hashimoto's thyroiditis.<sup>13,14</sup> Many reports demonstrate that AT is mainly a Th1-mediated autoimmune disease with a critical role played by IFN $\gamma$ .<sup>5,15,16</sup> In contrast, interleukin-4 (IL-4) positively regulates the Th2 immune response, including B cell activation and the development of thyroiditis, as well as autoantibody production rely on B lymphocytes.<sup>17</sup> IL-4 is known to repress the Th1 immune response, but its implication in autoimmune diseases remains unclear.<sup>18</sup> IL-4 can suppress autoimmune diabetes in transgenic NOD mice with pancreatic IL-4 expression,<sup>19</sup> whereas IL-4 treatment worsens the disease progression in models of colitis or uveoretinitis.<sup>20,21</sup> In an adoptive model of EAT, IL-4 incubation of spleen cells during mTg priming results in lower levels of TgAbs.<sup>22</sup> Conversely, IL-4 has been shown to increase the severity of granulomatous EAT.<sup>23</sup> Nevertheless, genetic invalidation of IFN $\gamma$  but not IL-4 protects the animals from SAT, demonstrating that IFN $\gamma$  is required for disease development.<sup>24</sup>

Recently, we have shown that thyroid IL-4 expression could mitigate hyperthyroidism in a mouse model of Graves' disease.<sup>25</sup> Knowing the antagonistic effect of IL-4 on the Th1 immune response, we have evaluated if the thyroid expression of IL-4 by thyrocytes (Thyr-IL4) could protect NOD.H2<sup>h4</sup> animals from accelerated SAT.

## Materials and Methods

### Animals

Thyr-IL4 C57BL/6J mice overexpressing the murine IL-4 have been described elsewhere.<sup>26</sup> NOD.H2<sup>h4</sup> mice<sup>27</sup> were kindly provided by Profs. Sandra McLachlan and Basil Rapoport. To generate Thyr-IL4 NOD.H2<sup>h4</sup> mice, transgenic animals were backcrossed to wild-type (WT) NOD.H2<sup>h4</sup> for at least six generations. Only N6 and N7 animals were used in the subsequent experiments. The majority of experiments were performed on the Thyr-IL4 NOD.H2<sup>h4</sup> line 52, and some results were reproduced in the independent transgenic line 30.

Both males and females were exposed to 0.05% sodium iodide (NaI; 217638; Sigma-Aldrich) in drinking water or regular water (control group) from age 8 weeks to accelerate SAT. Blood was collected from the retro-orbital plexus after 8 weeks and at the sacrifice of the mice (16 weeks). Animals were polymerase chain reaction (PCR) genotyped from mouse tail DNA using primers targeting the transgenic construct.<sup>26</sup> All animal experiments were conducted in accordance with the guidelines and approval of the Institutional Animal Care and Use Committee at the "Université libre de Bruxelles" (CEBEA permits 505N/649N). A conventional animal housing facility was used to breed the animals in regulated humidity, temperature, and light/dark room conditions. *Ad libitum* access to food and water was also provided.

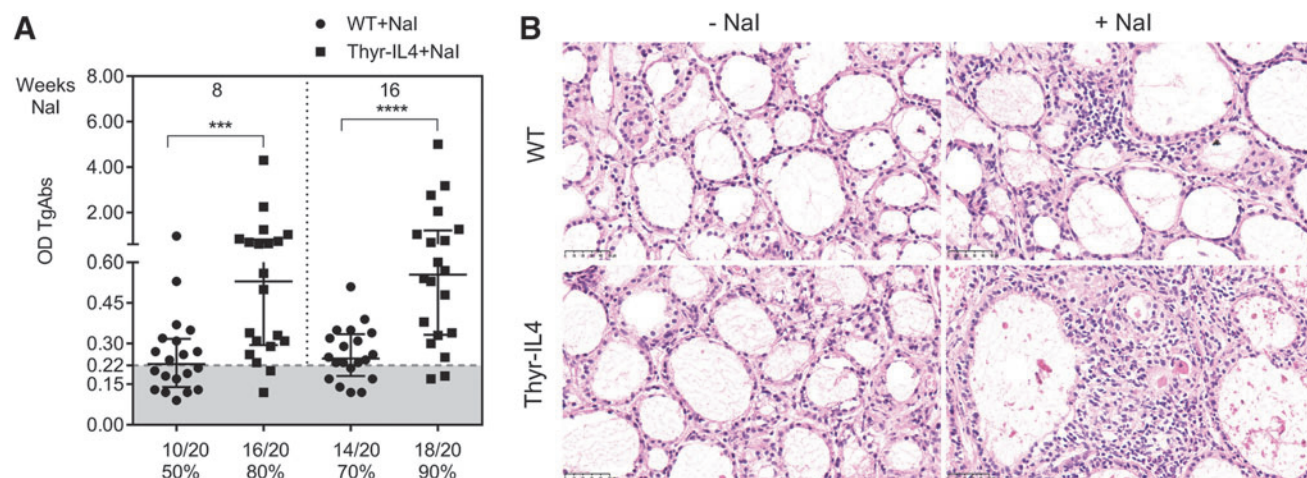


**FIG. 1.** Thyr-IL4 NOD.H2<sup>h4</sup> mice developed severe SAT after treatment with iodized drinking water (0.05% NaI). (A) Autoantibodies against mouse Tg (TgAbs) measured by ELISA (OD 490 nm) in WT and transgenic animals after 8 and 16 weeks of NaI. Values from individual animals are presented with the median and interquartile range. The dashed line represents the mean value + 2 SD for TgAb levels in control mice (-NaI; Thyr-IL4 [n=8] and WT [n=7]) as no significant difference was measured between WT and Thyr-IL4 animals on regular water. Animals with OD values higher than this upper limit are indicated as a percentage of the total number of mice in each group. *p* Values were calculated using Mann-Whitney *U* test. (B) Representative hematoxylin-eosin stained thyroid sections from WT and Thyr-IL4 mice exposed 16 weeks to NaI or regular water (-NaI). Magnification  $\times 40$  and scale bar: 50  $\mu$ m. \*\*\**p* < 0.001, \*\*\*\**p* < 0.0001. ELISA, enzyme-linked immunosorbent assay; NaI, sodium iodide; NOD.H2<sup>h4</sup>, nonobese diabetic; OD, optical densities; SAT, spontaneous autoimmune thyroiditis; SD, standard deviation; TgAbs, antibodies against thyroglobulin; Thyr-IL4, mouse model overexpressing IL-4 by thyrocytes; WT, wild-type.

### Enzyme-linked immunosorbent assay for autoantibodies to mouse Tg (TgAbs)

mTg was isolated from 30 to 35 thyroid lobes after homogenization in Dulbecco's phosphate-buffered saline (DPBS; supplemented with protease cocktail inhibitors (cOmplete Mini; Roche), filtrated through a 0.22  $\mu$ m filter (VWR) and purified on a size exclusion column HiLoad 16/600

(GE HealthCare) as previously described.<sup>28</sup> Enzyme-linked immunosorbent assay for TgAbs was performed on 96-well plates (3355; Thermo Scientific) coated with 1.5  $\mu$ g/mL mTg using sera (1:100 dilution) in duplicate.<sup>29</sup> Negative controls were sera from untreated young 8-week-old NOD.H2<sup>h4</sup> and C57BL/6 animals. Values are presented as optical densities (OD) at 490 nm of the tested sera subtracted from the blank value (without mouse serum).

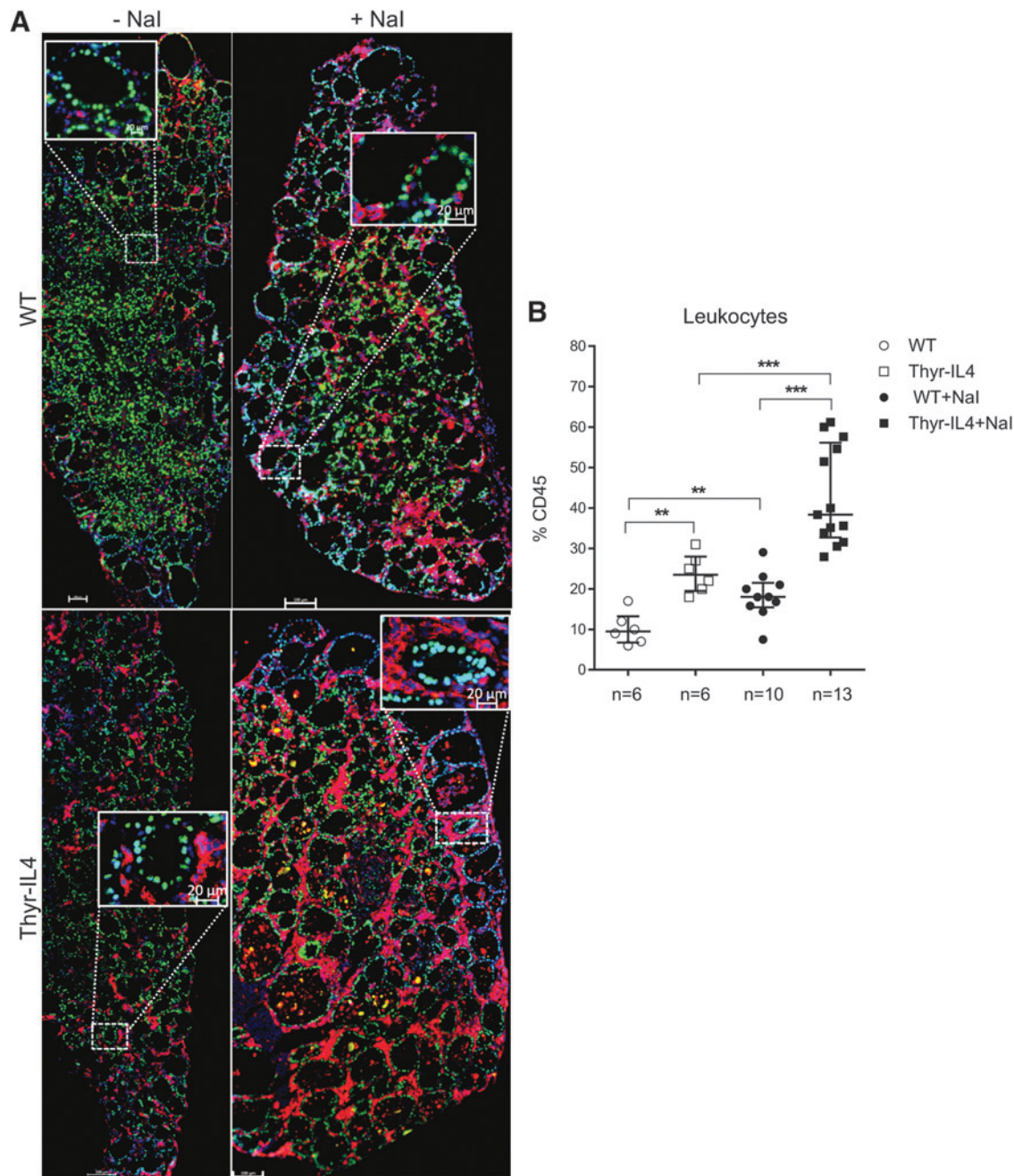


**FIG. 2.** Extensive leukocyte infiltrations are observed in the thyroids of Thy-IL4 NOD.H2<sup>h4</sup> mice. (A) Many CD45<sup>+</sup> cells are detected in Thy-IL4 animals after 16 weeks on NaI. Immunofluorescence staining on transgenic and WT thyroid sections using anti-NKX2.1 (green) and anti-CD45 (red) antibodies. Original magnification,  $\times 20$  for representative thyroid sections from each group (Scale bar: 100  $\mu$ m). The boxed area is magnified in the inset showing specific staining of CD45<sup>+</sup> cells, which are NKX2.1<sup>-</sup> (Scale bar: 20  $\mu$ m). (B) Percentage of leukocytes (number of CD45<sup>+</sup>/NKX2.1<sup>-</sup> cells divided by the total number of DAPI<sup>+</sup> cells) calculated in multiple samples with QuPath software on whole thyroid sections. Each dot represents the percentage of leukocytes in the thyroid of individual mice with the median and interquartile range. The numbers of mice studied in each group are indicated. \*\*p < 0.01, \*\*\*p < 0.001.



### Serum thyrotropin assay

Mouse serum thyrotropin (TSH) levels were measured with a TSH bioassay using stable JP26 CHO cells expressing the human TSH receptor.<sup>30</sup> cAMP was measured by radioimmunoassay, and data were expressed as picomoles of cAMP/50,000 cells.

### Thyroid histology procedures

Thyroid lobes were dissected and weighed before being frozen in Tissue-Tek optimal cutting temperature (4583 compound; Sakura). Thyroid blocks were sectioned at 5  $\mu$ m,

mounted on glass slides, and sections were stained with hematoxylin and eosin (Sigma-Aldrich) before being scanned with the NanoZoomer-SQ Digital Slide scanner (Hamamatsu).

For immunofluorescence staining, cryosections fixed in 4% paraformaldehyde were incubated in blocking solution (phosphate buffered saline containing 3% bovine serum albumin [Sigma-Aldrich], 5% horse serum [Invitrogen], and 0.3% Triton X-100 [Bio-Rad]) before incubation with primary antibodies: anti-CD106 (Vascular Cell Adhesion Molecule-1 [VCAM-1]; 550547; BD Pharmingen), anti-CD62E (E-selectin; 553749; BD Pharmingen), anti-CD4 (GK1.5 14-0041-82; Invitrogen), anti-CD8 (GK1.5 14-0081-82;

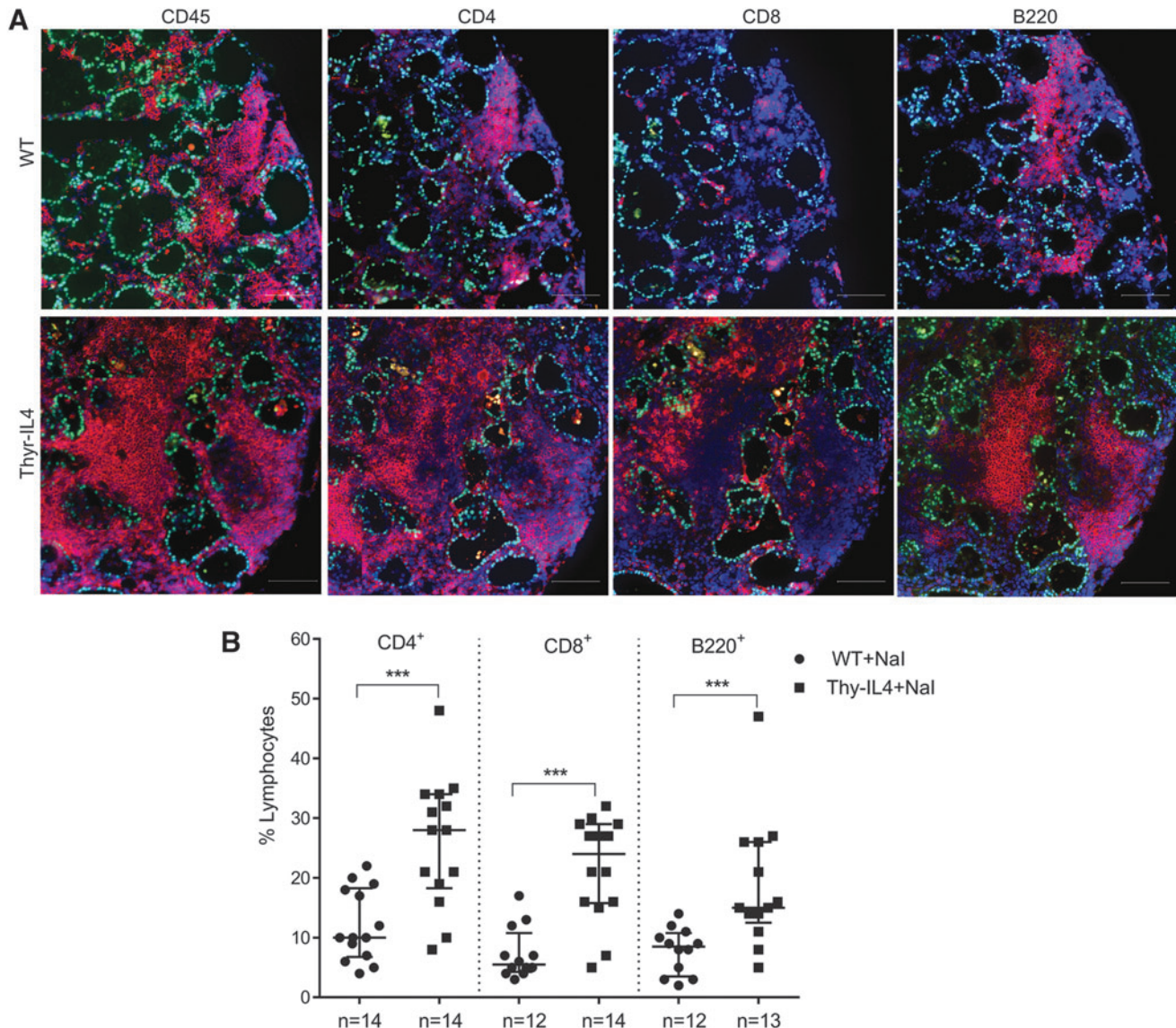


**FIG. 3.** Characterization of T and B cell populations in the thyroids of WT and Thy-IL4 NOD.H2<sup>h4</sup> mice exposed 16 weeks to iodized water. (A) Immunofluorescence staining was carried out on serial sections using anti-CD45, anti-CD4, anti-CD8, or anti-B220 (red) with anti-NKX2.1 (green) antibodies. WT and Thy-IL4 mice showed many clustered CD4<sup>+</sup> T+B220<sup>+</sup> B cells, forming aggregates more frequently observed in transgenic animals. The CD8<sup>+</sup> T cells were scattered throughout the tissue of Thy-IL4 mice, and fewer CD8<sup>+</sup> cells were present in WT mice. Original magnification,  $\times 20$  (scale bar: 100  $\mu$ m). (B) Percentage of lymphocytes (number of CD4<sup>+</sup> or CD8<sup>+</sup> or B220<sup>+</sup> and NKX2.1<sup>-</sup> cells divided by the total number of DAPI<sup>+</sup> cells) calculated in multiple samples with QuPath software on whole thyroid sections (see Materials and Methods section). Scatter plots show the median with the interquartile range; each dot represents the percentage of lymphocytes in the thyroid of individual mice. The numbers of mice studied in each group are indicated. \*\*\* $p < 0.001$ .

Invitrogen), anti-B220 (FP10422050; MBL), and anti-CD45 (30F11; BioLegend) with anti-NKX2.1 antibody (ab76013; Abcam). After washing, the tissues were incubated with two secondary antibodies: anti-rabbit Alexa Fluor 488 (A21206; Invitrogen) and anti-rat Rhodamine Red-X (712-295-150; Jackson) and nuclei stained with DAPI (D9564; Sigma-Aldrich). The images were acquired on a Zeiss Axio Imager Zoom V16 microscope (Carl Zeiss) using a  $\times 20$  magnification and analyzed with Zen 3.3 (Blue edition) Software. Percentage of positive cells was calculated in multiple samples with QuPath software on whole thyroid cryosections.<sup>31</sup>

#### Real-time quantitative PCR

Total RNA was extracted from one thyroid lobe using the RNeasy Mini Kit (HB-0435; Qiagen). After DNase treatment, 1  $\mu$ g of total RNA was reverse-transcribed with Superscript II reverse-transcriptase (Invitrogen). Real-time quantitative PCR was performed using KAPA Fast SYBR Green (Kapa Biosystems) on a C1000 Touch Thermal Cycler CFX96 Real-Time System (Bio-Rad) with gene-specific, intron-spanning primers (Supplementary Table S1). Relative

RNA expressions were analyzed with the Pfaffl method after normalization to Retention Endoplasmic Reticulum 1 homolog (*RER1*) and TATA-box Binding Protein (*TBP*) genes.<sup>32,33</sup> Primer sequences were selected to target the 5' untranslated region of the IL-4 transcript to amplify selectively the endogenous IL-4 isoform.

#### Flow cytometry

Immediately after dissection, single-cell suspensions were prepared from individual mouse thyroid, immunostained, and analyzed on a FACS BD LSRFortessa™ (BD Biosciences) (Supplementary Methods S1).

#### Statistical analyses

Statistical analyses were achieved using the Mann–Whitney *U* test (GraphPad Prism 6.0 software; GraphPad Software, Inc., San Diego, CA). Values were considered significant at  $*p < 0.05$ ,  $**p < 0.01$ ,  $***p < 0.001$ ,  $****p < 0.0001$ , and the data of individual mice were presented in the graphs with the median and interquartile range.

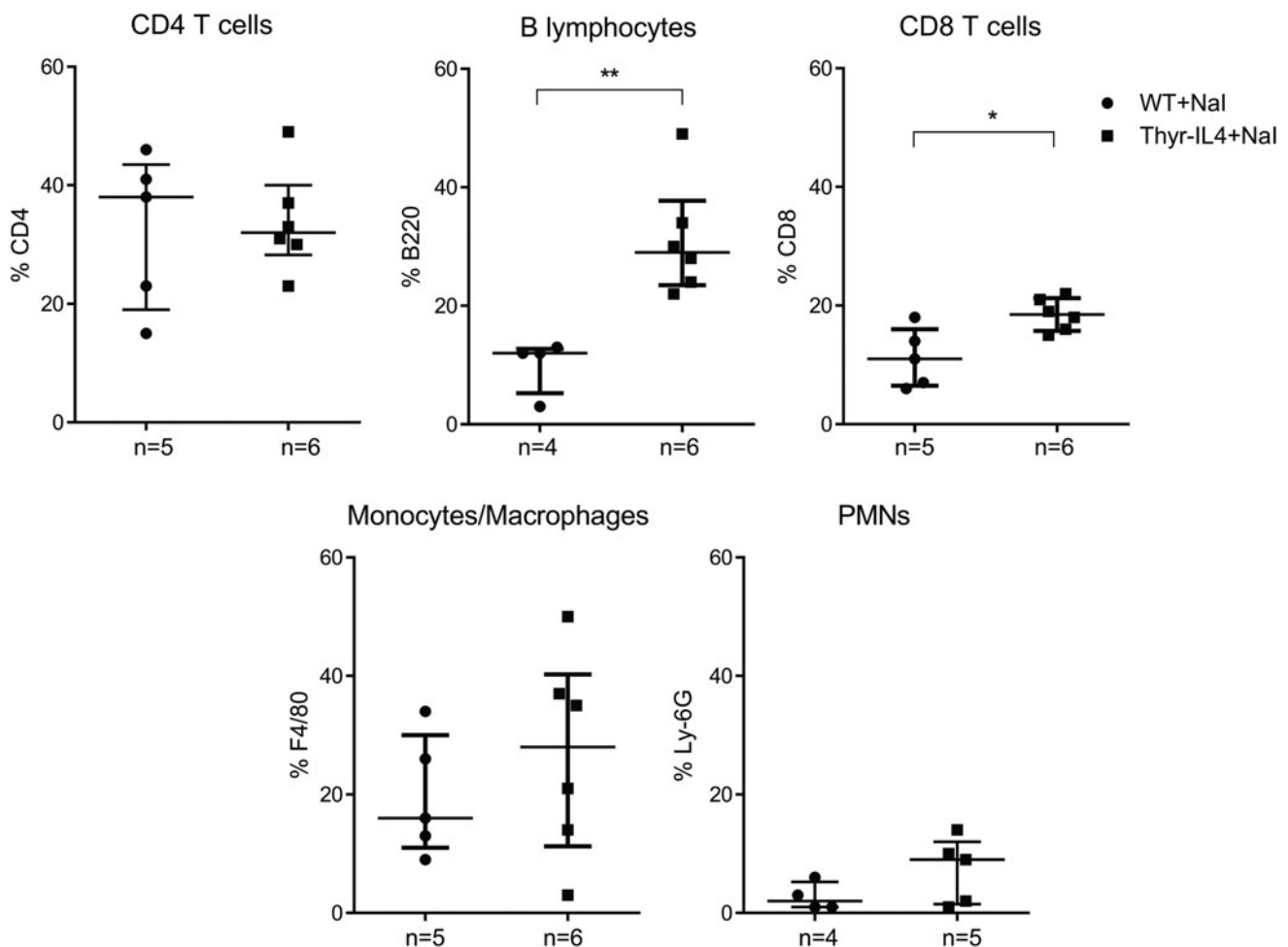


**FIG. 4.** CD45<sup>+</sup> immune cell distribution in thyroid infiltrates by flow cytometry. Thyroid single cell suspensions from 16 weeks of NaI treated WT and Thy-IL4 NOD.H2<sup>h4</sup> animals were stained with the respective fluorescent-labeled antibodies. CD45<sup>+</sup> vs. immune cells (CD4, CD8, F4/80, Ly-6G, and B220) were plotted after gating on the intact cell population (DAPI<sup>+</sup> cells). The CD4, CD8, F4/80, LY-6G, and B220 immune cell populations are presented as a percentage of the total number of CD45<sup>+</sup> cells. The numbers of mice studied in each group are indicated.  $*p < 0.05$ ,  $**p < 0.01$ .

## Results

### Severe accelerated SAT in *Thyr-IL4* *NOD.H2<sup>h4</sup>* animals

WT and *Thyr-IL4* *NOD.H2<sup>h4</sup>* animals were treated with sodium-iodized water (0.05% NaI) during 8 and 16 weeks. Circulating TgAbs were constantly more elevated in *Thyr-IL4* animals relative to WT after exposure to NaI. A higher number of transgenic animals presented this increase, although the incidence did not reach statistical significance (Fig. 1A). Consistent with TgAb titers, the severity of accelerated SAT was markedly enhanced in *Thyr-IL4* with multiple foci of mononuclear cell infiltrates throughout the thyroid parenchyma, replacing the normal thyroid architec-

ture in some transgenic animals (Fig. 1B). Anti-CD45 immunostaining confirmed the presence of numerous leukocytes in the thyroid of WT and *Thyr-IL4* animals after 16 weeks of NaI treatment (Fig. 2A). Quantitatively, the percentage of CD45<sup>+</sup> cells in treated mice was drastically increased in transgenic (38%) relative to WT (18%) animals (Fig. 2B). Moreover, age matched *Thyr-IL4* animals under regular water displayed also more frequent intrathyroidal leukocytes relative to WT littermates.

Upregulation of the endothelial activation markers VCAM-1 and E-selectin was also enhanced in the thyroids of NaI treated *Thyr-IL4* mice (Supplementary Fig. S1). As previously reported in WT *NOD.H2<sup>h4</sup>*,<sup>34</sup> we found that the majority of CD45<sup>+</sup> cells encompassed CD4<sup>+</sup> T lymphocytes

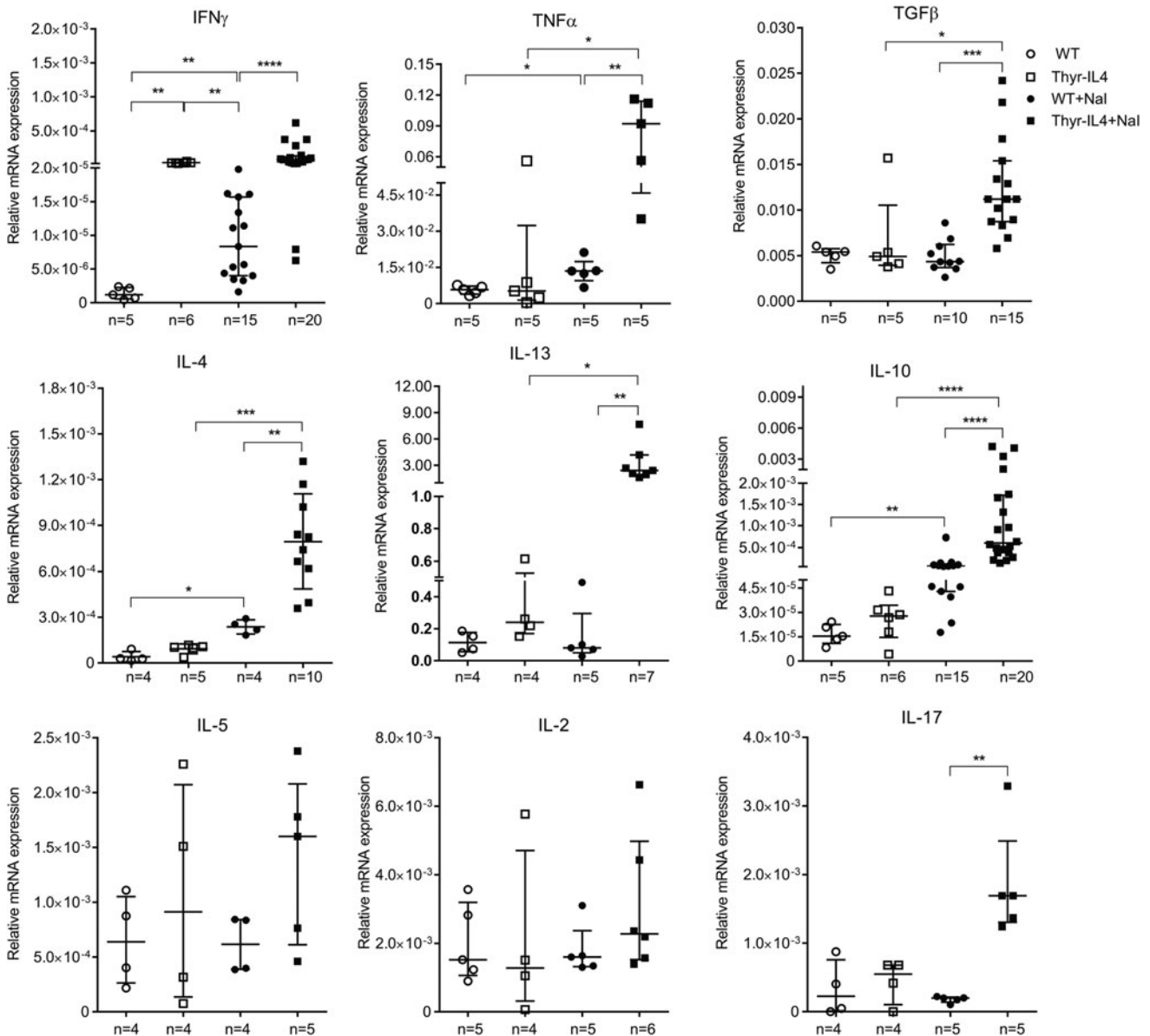


**FIG. 5.** Intrathyroidal cytokine mRNA expression in *NOD.H2<sup>h4</sup>* mice. Relative mRNA expression of cytokines was determined by RT-qPCR in thyroids collected after 16 weeks of NaI treatment. The data are presented by median with interquartile range. IL-4 corresponds to the endogenous IL-4 isoform mRNA. The numbers of mice studied in each group are indicated. IL-4, interleukin-4; mRNA, messenger RNA; RT-qPCR, real-time quantitative polymerase chain reaction. \* $p < 0.05$ , \*\* $p < 0.01$ , \*\*\* $p < 0.001$ , \*\*\*\* $p < 0.0001$ .



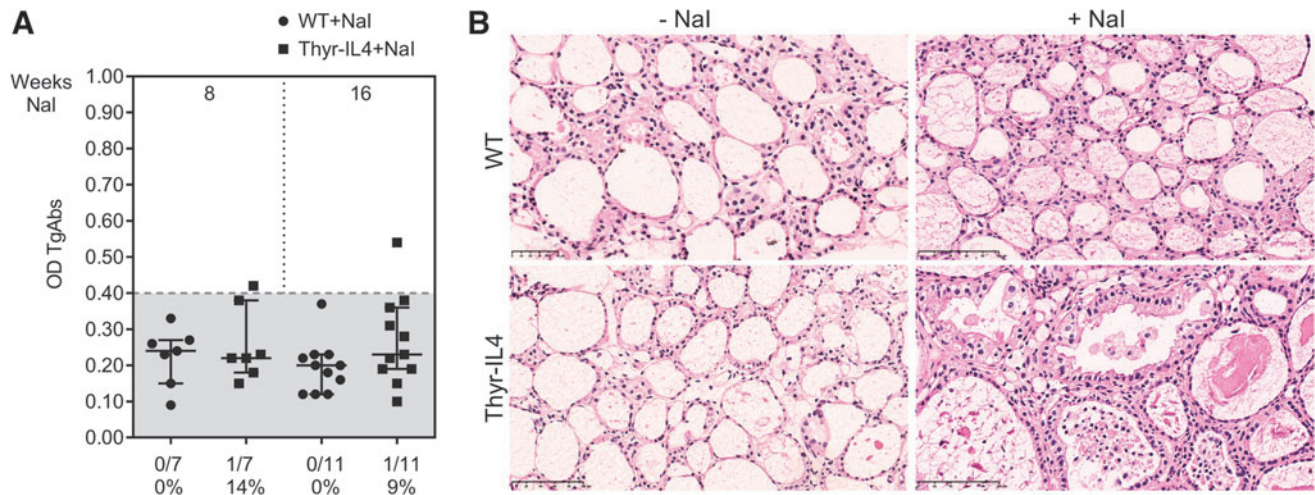


**FIG. 6.** Thy-IL4 C57BL/6 mice developed large thyroid leukocyte infiltrations in absence of elevated TgAbs after 16 weeks on iodized water (NaI). (A) TgAbs in WT and transgenic animals after 8 and 16 weeks of NaI measured by ELISA (OD 490 nm). Values from individual animals are presented with the median and interquartile range. The dashed line represents the mean value +2 SD for TgAb levels in control mice (-NaI; Thy-IL4 [ $n=4$ ] and WT [ $n=5$ ]) as no significant difference was measured between WT and Thy-IL4 animals on regular water. Animals with OD values higher than this upper limit are indicated as a percentage or a fraction of the total number of mice in each group. (B) Representative hematoxylin-eosin stained thyroid sections from WT and Thy-IL4 mice exposed 16 weeks to NaI or standard water (-NaI). Magnification  $\times 40$  and scale bar: 50  $\mu\text{m}$ .

and B220<sup>+</sup> B cells forming lymphoid clusters, while CD8<sup>+</sup> T cells were more scattered in the thyroid tissue (Fig. 3A). This inflammatory cell distribution was conserved in transgenic treated animals, although the respective cellular populations were all significantly enhanced (Fig. 3B), reflecting the intense thyroid inflammation. After antibody staining and gating on intact cells, the different immune cell populations were identified by flow cytometry as a percentage of the total number of CD45<sup>+</sup> cells (Supplementary Fig. S2). At the end of the NaI treatment, the leukocyte population infiltrating the thyroid of Thy-IL4 mice was significantly enriched in CD8<sup>+</sup> T and B220<sup>+</sup> B lymphocytes (Fig. 4).

Finally, the messenger RNA (mRNA) expression of the main Th1 and Th2 cytokines was quantified in the thyroid lobes of animals 16 weeks after receiving regular or iodide-supplemented water (Fig. 5). As expected, excessive iodide supply of WT NOD.H2<sup>h4</sup> moderately induced the expression of IFN $\gamma$ , TNF $\alpha$ , IL-4, and IL-10.<sup>10</sup> Consistent with the substantial thyroid infiltrate, the expression of TNF $\alpha$ , IL-4, and IL-10 was considerably augmented in NaI treated Thy-IL4

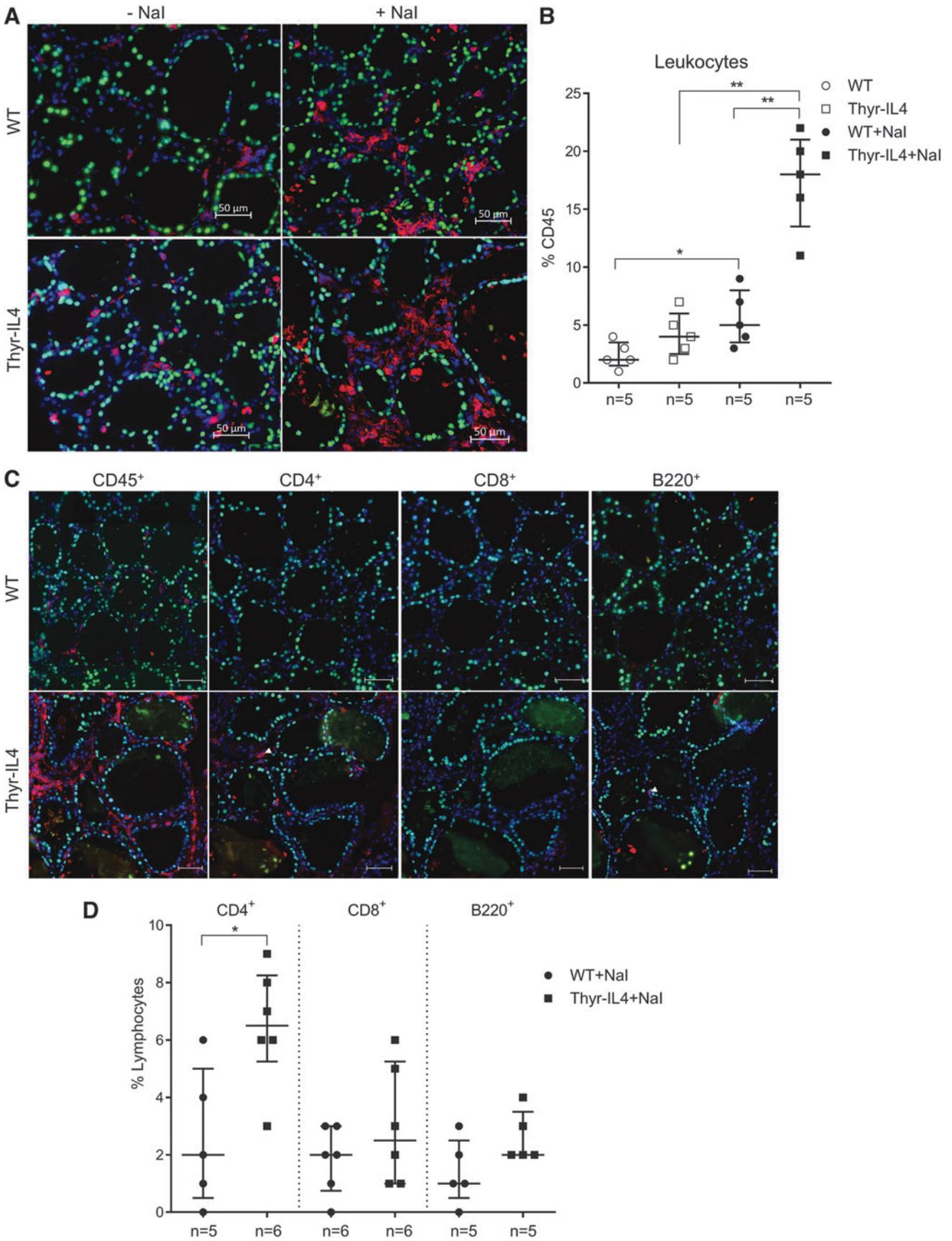
animals, as well as TGF $\beta$ , IL-13, and IL-17. Accumulation of Th17 cells was reported in the thyroid of NOD.H2<sup>h4</sup> animals, and IL-17<sup>-/-</sup> animals develop reduced iodide-induced SAT lesions.<sup>35</sup> Surprisingly, thyroid expression of IFN $\gamma$  was already elevated in transgenic mice receiving regular water and was not statistically augmented after accelerated SAT. These data were reproduced in the second independent Thy-IL4 NOD.H2<sup>h4</sup> line 30 (Supplementary Fig. S3).

These findings demonstrated that ectopic expression of IL-4 by TFCs increased the severity of iodide-induced SAT lesions with large lymphocytic infiltrations and could influence the composition and/or the activation of the immune cells infiltrating the inflamed tissue.

#### Thyroid inflammation in SAT-resistant Thy-IL4 C57BL/6 animals on iodized water

Compared to disease-prone NOD.H2<sup>h4</sup> animals, virtually none of the parental C57BL/6 presented elevated TgAbs after

**FIG. 7.** Intrathyroidal immune cell populations observed in treated Thy-IL4 C57BL/6 mice were different from NOD.H2<sup>h4</sup>. (A) Many CD45<sup>+</sup> cells are detected in Thy-IL4 animals after 16 weeks on NaI. Immunofluorescence staining on thyroid sections using anti-NKX2.1 (green) and anti-CD45 (red) antibodies. Original magnification,  $\times 20$  for representative thyroid sections from each group (scale bar: 50  $\mu\text{m}$ ). (B) Percentage of leukocytes (number of CD45<sup>+</sup>/NKX2.1<sup>-</sup> cells divided by the total number of DAPI<sup>+</sup> cells) calculated in multiple samples with QuPath software on whole thyroid sections. Each dot represents the percentage of leukocytes in the thyroids of individual mice with the median and interquartile range. The numbers of mice studied in each group are indicated below. (C) Immunofluorescence staining of T and B cell populations carried out on serial sections from animals on iodized water for 16 weeks using anti-CD45, anti-CD4, anti-CD8, or anti-B220 (red) with anti-NKX2.1 (green) antibodies. The majority of CD45<sup>+</sup> cells in the thyroid infiltrates observed in Thy-IL4 mice after NaI exposition are not T or B lymphocytes. Original magnification,  $\times 20$  and scale bar: 100  $\mu\text{m}$ . (D) Percentage of lymphocytes among the total number of DAPI<sup>+</sup> cells calculated in multiple samples with QuPath software on whole thyroid sections. Scatter plots show the median with the interquartile range, each dot represents the percentage of lymphocytes in the thyroids of individual mice. The numbers of mice studied in each group are indicated. \* $p < 0.05$ , \*\* $p < 0.01$ .





8 or 16 weeks on iodized-supplemented water (Fig. 6A). Unexpectedly, moderate mononuclear infiltrates were evident in the thyroids of transgenic mice at the end of the treatment (Fig. 6B). Immunostaining confirmed the leukocytic nature of the thyroid infiltrate, with quantitatively more CD45<sup>+</sup> cells in Thyr-IL4 animals (18%) relative to WT littermates (5%) on NaI (Fig. 7A, B). Notably, these infiltrating cells could penetrate into the colloidal lumen of transgenic thyroids. Contrary

to NOD.H2<sup>b4</sup> mice, immunophenotyping of these immune cells on serial sections revealed that a very limited number of leukocytes were positives for CD4, CD8, or B220 (Fig. 7C). Only the frequency of CD4<sup>+</sup> T cells among total intrathyroidal cells (DAPI<sup>+</sup>) was slightly but significantly augmented in Thyr-IL4 thyroids after the treatment (Fig. 7D).

While the induction of intrathyroidal TNF $\alpha$ , TGF $\beta$ , IL-4, and IL-13 was reproduced in Thyr-IL4 C57BL/6 relative to

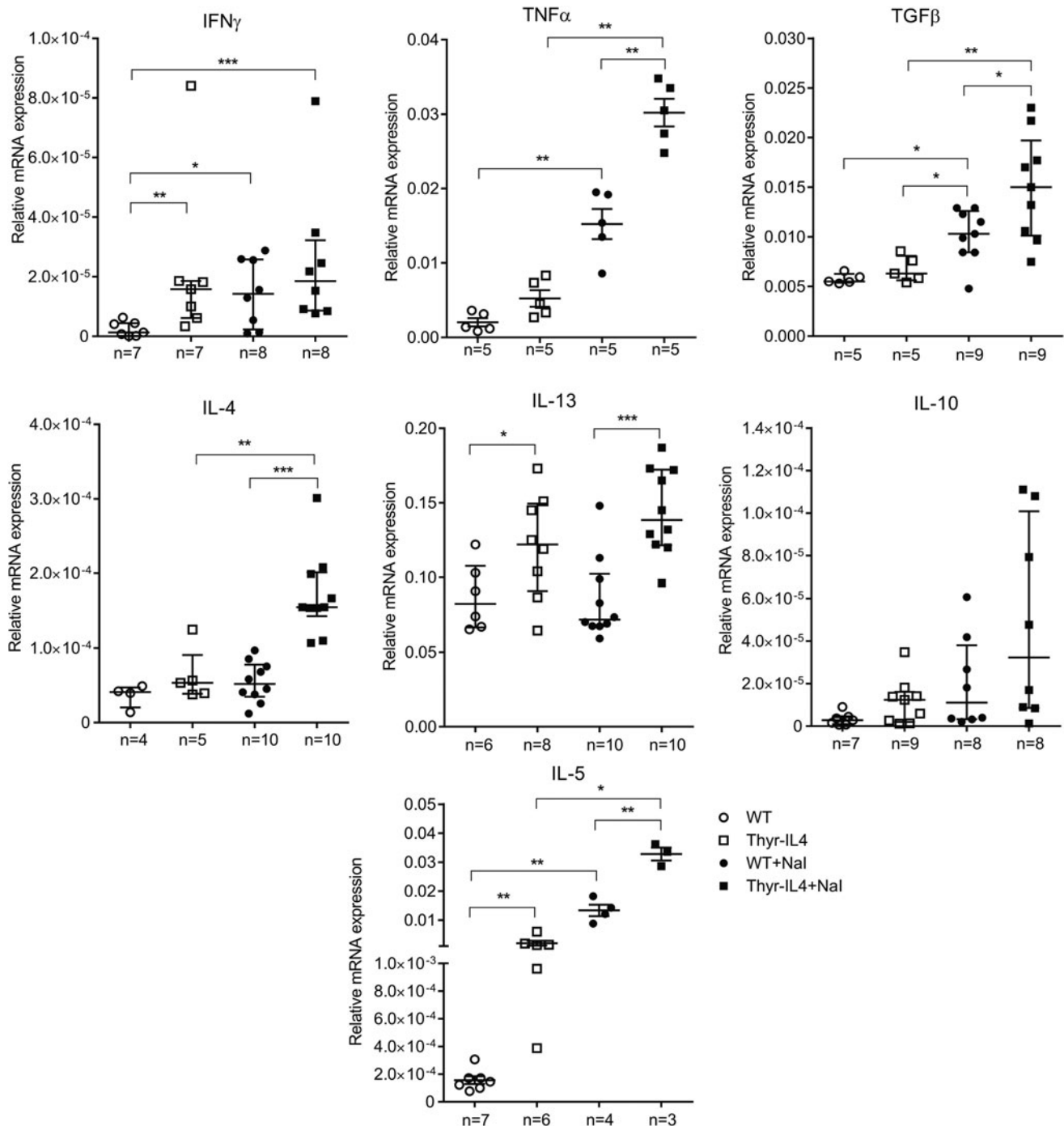


**FIG. 8.** Intrathyroidal cytokine mRNA expression in C57BL/6 mice. Relative mRNA expression of cytokines was determined by RT-qPCR on thyroids collected after 16 weeks on iodized water. The data are presented by median with interquartile range. IL-4 corresponds to the endogenous IL-4 isoform mRNA. The numbers of mice studied in each group are indicated. \* $p < 0.05$ , \*\* $p < 0.01$ , \*\*\* $p < 0.001$ .

WT mice after NaI exposure, no significant induction of IFN $\gamma$  or IL-10 could be measured (Fig. 8). Transgenic animals on regular water presented also elevated expression of IL-13 and IFN $\gamma$  compared to WT. The major difference between the two mouse strains concerned IL-5, which was not modulated in the SAT-prone NOD.H2<sup>h4</sup> model, but clearly induced in the thyroids of NaI treated WT and transgenic C57BL/6 mice. We quantified the levels of some circulating cytokines in the serum of NOD.H2<sup>h4</sup> and C57BL/6 treated animals (Supplementary Fig. S4). Despite some significant modulations observed, no definitive conclusion could be drawn due to the limited sensitivity of the method. Nevertheless, over-expression of circulating IL-4 was noticeably detected in the serum of all Thyr-IL4 animals.

All these data demonstrated that a constitutive expression of IL-4 by the thyrocytes could induce non-AT after high iodide intake in SAT-resistant C57BL/6 animals.

#### Altered thyroid function in Thyr-IL4 animals on iodized-supplemented water

In contrast to WT animals, both NaI-treated Thyr-IL4 strains developed marked thyroid enlargement associated with elevated circulating TSH levels and lower serum T4 (Fig. 9, Supplementary Fig. S5 and data not shown). Non-transgenic animals showed normal thyroidal *Nis* down-regulation after 16 weeks of NaI supply, demonstrating their capacity to escape the Wolff-Chaikoff block to resume TH

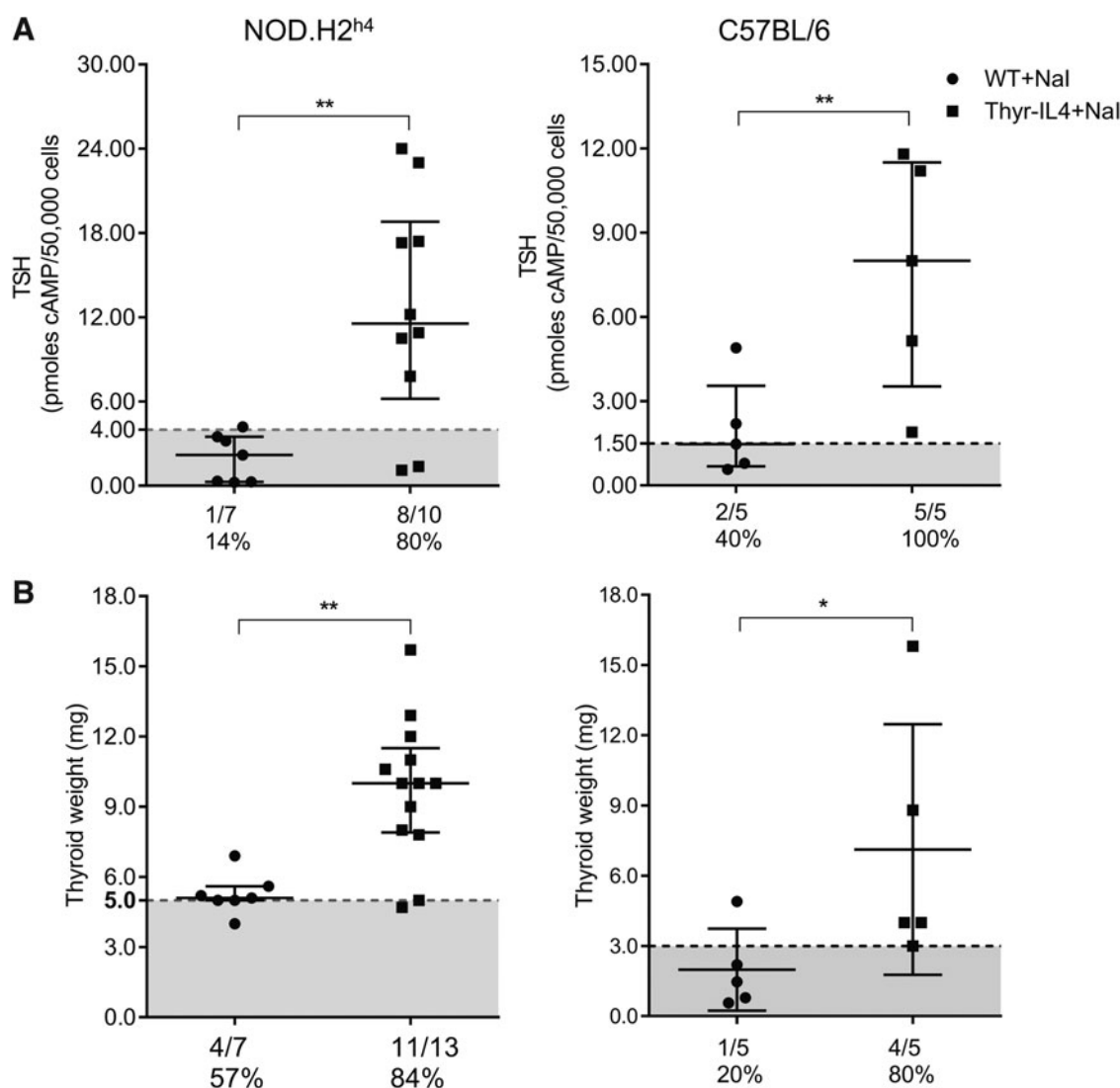


**FIG. 9.** Altered thyroid function in Thyr-IL4 males exposed to iodized water. (A) Serum TSH levels measured by bioassay (pmol cAMP produced by 50,000 TSHR-expressing cells) in NOD.H2<sup>h4</sup> and C57BL/6 males treated for 16 weeks. The dashed line represents the mean value +2 SD for TSH levels in control mice (-NaI; NOD.H2<sup>h4</sup> Thyr-IL4 [ $n=8$ ] and WT [ $n=6$ ]; C57BL/6 Thyr-IL4 [ $n=3$ ] and WT [ $n=3$ ]) as no significant difference was measured between WT and Thyr-IL4 animals on regular water. (B) Weights of thyroid lobes from individual animals. The dashed line represents the mean value +2 SD for thyroid weights of control mice (-NaI; NOD.H2<sup>h4</sup> Thyr-IL4 [ $n=8$ ] and WT [ $n=6$ ]; C57BL/6 Thyr-IL4 [ $n=5$ ] and WT [ $n=5$ ]). Animals with values higher than the upper limit are indicated as a percentage or a fraction of the total number of mice in each group. \* $p < 0.05$ , \*\* $p < 0.01$ . TSH, thyrotropin.

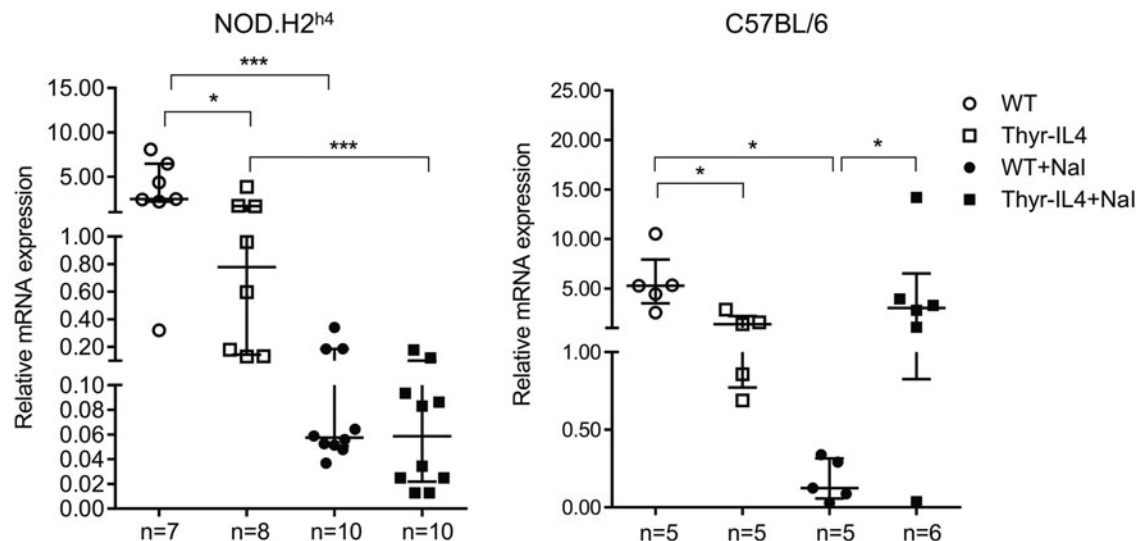


**FIG. 10.** Relative expression of *Nis* mRNA in NOD.H2<sup>h4</sup> and C57BL/6 mice treated for 16 weeks (+NaI) or not with iodized water. The number of mice is presented under each group. The values of individual mice that are presented in the graphs and median with interquartile range are shown. \* $p < 0.05$ , \*\*\* $p < 0.001$ .

synthesis<sup>12,36</sup> (Fig. 10). This degree of *Nis* repression was similar in Thy-IL4 NOD.H2<sup>h4</sup> despite their severe hypothyroid phenotype. In contrast, *Nis* expression was inappropriately preserved in Thy-IL4 C57BL/6 animals compared to WT littermates, suggesting a failure in limiting iodide uptake in the thyroid.

## Discussion

Meta-analyses have revealed some significant associations between *IL-4* genetic variants and the risk to develop autoimmune thyroid diseases.<sup>37,38</sup> Based on the ability of IL-4 to counteract the Th1 immune response, it has been proposed that it could be used as a therapeutic agent to treat autoimmune pathologies.<sup>39</sup> Using Thy-IL4 animals, we explored whether a thyroid expression of IL-4 could fulfill this assumption in the context of AT. However, we have clearly demonstrated that Thy-IL4 NOD.H2<sup>h4</sup> developed severe SAT lesions after excessive iodide ingestion. Thyroid inflammation in NOD.H2<sup>h4</sup> animals has been well documented.<sup>40</sup> The infiltrate is mainly composed of CD4<sup>+</sup>, CD8<sup>+</sup>, and B220<sup>+</sup> lymphocytes associated with elevation of thyroid Th1/Th2 cytokine expression,<sup>10,34</sup> and all these SAT hallmarks were exacerbated in treated Thy-IL4 NOD.H2<sup>h4</sup> animals. The leukocyte enrichment in CD8<sup>+</sup> T and B lymphocytes could explain the massive thyroid destruction with high TgAbs observed in Thy-IL4 mice. However, we cannot exclude that the artificial thyroid expression of the IL-4 transgene would be responsible for this unexpected phenotype.

The major limitation of this study is the absence of mechanisms by which IL-4 enhances thyroiditis. The present data might seem somewhat inconsistent with previous studies showing that *IL-4* knockout (KO) NOD.H2<sup>h4</sup> normally developed accelerated SAT.<sup>24</sup> However, the published data did not exclude a role of IL-4 during the disease progression. Similar unreliable findings were reported in NOD.H2<sup>h4</sup> mice with thyroid expression of IFN $\gamma$ . Actually, Thy-IFN $\gamma$  animals were protected against SAT, which was unexpected

considering the decisive role of this cytokine in AT.<sup>41,42</sup> In Thy-IL4 mice, local accumulation of IL-4 could improve the capacity of autoreactive B cells to respond to thyroid autoantigens. Moreover during SAT progression in WT NOD.H2<sup>h4</sup>, elevation of thyroidal IL-4 is only detected late in the disease<sup>10</sup> with endothelial induction of VCAM-1<sup>43</sup> known to be regulated by IL-4.<sup>44</sup> Therefore, the precocious thyroid expression of IL-4 in Thy-IL4 mice could also facilitate the leukocyte infiltration by early VCAM-1 induction (Supplementary Fig. S1).

Expression of the Intracellular Adhesion Molecule-1 (ICAM-1) was shown on thyrocytes from Hashimoto's patients and positively regulated by IL-4 in bronchial and colonic epithelial cells.<sup>45-47</sup> The corresponding IL-4 receptor being expressed in TFCs,<sup>48</sup> it is possible that IL-4 could also mediate ICAM-1 expression in Thy-IL4 mice promoting thyroid inflammation. Furthermore, the systemic humoral immune response in transgenic animals could be improved by the elevated IL-4 serum levels.

A second consequence of the ectopic IL-4 overexpression in absence of NaI treatment was the Th1 polarization of leukocytes infiltrating the transgenic thyroid tissue illustrated by the intrathyroidal increase of IFN $\gamma$ . IL-4 is able to accelerate Th1-mediated colitis with upregulation of IFN $\gamma$  in the intestine.<sup>20</sup> Thyrocytes from Hashimoto's patients present IFN $\gamma$ -induced major histocompatibility complex (MHC) II that is repressed in IFN $\gamma$  KO NOD.H2<sup>h4</sup>.<sup>24,49</sup> In addition, IFN $\gamma$  acts synergistically with iodine to increase the expression of ICAM-1 on thyrocytes of NOD.H2<sup>h4</sup>, suggesting that ICAM-1 could be a key disease susceptibility factor.<sup>42</sup> Further experiments with blocking antibodies would help to discriminate the respective role of IL-4 and IFN $\gamma$  in Thy-IL4 NOD.H2<sup>h4</sup> accelerated SAT.

In contrast to NOD.H2<sup>h4</sup> presenting the MHC haplotype H<sup>2k</sup>, excessive iodide intake does not induce AT in C57BL/6 having the MHC haplotype H.<sup>2b,12,50</sup> Surprisingly, a significant number of treated Thy-IL4 C57BL/6 developed substantial mononuclear thyroid infiltrates. However, this was not



associated with elevated TgAbs, suggesting that the thyroid or systemic expression of IL-4 was not sufficient to trigger autoimmunity in C57BL/6. A similar phenotype was observed in C57BL/6 with thyroid expression of the chemokine CCL21 that present large lymphocytic thyroid lesions without TgAbs.<sup>51</sup>

Nevertheless, our findings support a role of IL-4 in NaI-induced thyroid inflammation. Similar to Thy-IL4 NOD.H2<sup>h4</sup>, thyroid elevation of Th1 and Th2 cytokines was measured. However, the limited number of CD4<sup>+</sup>, CD8<sup>+</sup>, and B lymphocytes found in the leukocyte infiltrates and the marked IL-5 increase suggested a different disease etiology in transgenic C57BL/6 with a SAT-resistant genetic background. IL-5 implication in AT is still unclear with only few studies reporting an elevation of serum IL-5 in Hashimoto's patients.<sup>52,53</sup> Further experiments should be conducted to better characterize the immune cell population in Thy-IL4 C57BL/6 mice.

Patients with subclinical thyroid disorders, like Hashimoto's thyroiditis, could develop hypothyroidism after excessive iodine ingestion.<sup>3</sup> However, the various mouse models generated to study AT do not frequently develop hypothyroidism.<sup>7,11,29,51</sup> In contrast, our transgenic animals present iodide-induced thyroid inflammation concomitant with primary hypothyroidism. Hence, they constitute a new valuable tool to better characterize the pathophysiology of this autoimmune thyroid disease.

It is commonly accepted that inflammatory cytokines negatively affect the thyroid function, including *NIS* inhibition.<sup>54</sup> In addition, impairment to reduce the excessive iodide intake through the Wolff–Chaikoff escape phenomenon could also result in hypothyroidism.<sup>55</sup> The thyroid dysfunction in transgenic C57BL/6 mice could be caused by the failure to reduce iodide excess associated with inflammatory cytokines produced locally in the inflamed tissue. The inappropriate preservation of *Nis* expression could be linked to the moderate inflammation preserving the TFC response to elevated TSH levels that may counterbalance *Nis* down-regulation. In contrast, the large thyroid lesions in Thy-IL4 NOD.H2<sup>h4</sup> could most probably provoke TH synthesis defect as observed in the final evolution of Hashimoto's thyroiditis characterized by the destruction and fibrous replacement of TFCs.

In conclusion, our findings demonstrated that expression of IL-4 by thyrocytes enhanced the severity of accelerated SAT in Thy-IL4 NOD.H2<sup>h4</sup> animals and promoted leukocyte infiltrations in the thyroid of SAT-resistant transgenic C57BL/6 mice. Moreover, disease development in both transgenic strains was associated with the emergence of a substantial hypothyroidism.

## Acknowledgments

The authors gratefully acknowledge Profs. Basil Rapoport and Sandra McLachlan (Thyroid Autoimmune Disease Unit, Cedars-Sinai Research Institute, Los Angeles, CA) for providing the NOD.H2<sup>h4</sup> mice and their continuous interest and judicious advice in the present study. The authors thank Jean-Marie Vanderwinden for the use of the microscope facility. Special thanks to Sang Van Tran for its excellent technical assistance.

## Authors' Contributions

K.M., F.M., and X.D.D. designed the project, and K.M. performed all the experiments. S.D. participated in some part of the project involving the manipulation of the mice. X.D.D. wrote the article. K.M., J.-E.D., and F.M. helped and edited the article. X.D.D. provided conceptual advice. All coauthors have approved the article for submission.

## Author Disclosure Statement

All the authors have no conflicts of interests to disclose.

## Funding Information

This work was supported by the “Fonds de la Recherche Scientifique” (FRS-FNRS; Grant Nos. J002114F–J005918F) and the Fund Doctor J.P. Naets, managed by the King Baudouin Foundation.

## Supplementary Material

Supplementary Methods S1  
Supplementary Table S1  
Supplementary Figure S1  
Supplementary Figure S2  
Supplementary Figure S3  
Supplementary Figure S4  
Supplementary Figure S5

## References

1. Dai G, Levy O, Carrasco N. Cloning and characterization of the thyroid iodide transporter. *Nature* 1996;379(6564): 458–460; doi: 10.1038/379458a0
2. Burek CL, Rose NR. Autoimmune thyroiditis and ROS. *Autoimmun Rev* 2008;7(7):530–537; doi: 10.1016/j.autrev.2008.04.006
3. Burek CL, Talor MV. Environmental triggers of autoimmune thyroiditis. *J Autoimmun* 2009;33(3–4):183–189; doi: 10.1016/j.jaut.2009.09.001
4. Jacobson DL, Gange SJ, Rose NR, et al. Epidemiology and estimated population burden of selected autoimmune diseases in the United States. *Clin Immunol Immunopathol* 1997;84(3):223–243; doi: 10.1006/CLIN.1997.4412
5. Rapoport B, McLachlan SM. Thyroid autoimmunity. *J Clin Invest* 2001;108(9):1253–1259; doi: 10.1172/JCI200114321
6. Quarantino S. Models of autoimmune thyroiditis. *Drug Discov Today Dis Model* 2004;1(4):417–423; doi: 10.1016/j.ddmod.2004.11.006
7. Ng HP, Banga JP, Kung AWC. Development of a murine model of autoimmune thyroiditis induced with homologous mouse thyroid peroxidase. *Endocrinology* 2004;145(2): 809–816; doi: 10.1210/en.2003-0656
8. Dai YD, Rao VP, Carayanniotis G. Enhanced iodination of thyroglobulin facilitates processing and presentation of a cryptic pathogenic peptide. *J Immunol* 2002;168(11):5907–5911; doi: 10.4049/JIMMUNOL.168.11.5907
9. Rasooly L, Burek CL, Rose NR. Iodine-induced autoimmune thyroiditis in NOD-H-2h4 mice. *Clin Immunol Immunopathol* 1996;81(3):287–292; doi: 10.1006/clin.1996.0191
10. Braley-Mullen H, Sharp GC, Medling B, et al. Spontaneous autoimmune thyroiditis in NOD.H-2h4 mice. *J Autoimmun* 1999;12(3):157–165; doi: 10.1006/jaut.1999.0272

11. Yu S, Sharp GC, Braley-Mullen H. Thyroid epithelial cell hyperplasia in IFN- $\gamma$  deficient NOD.H-2h4 mice. *Clin Immunol* 2006;118(1):92–100; doi: 10.1016/j.clim.2005.07.013
12. McLachlan SM, Aliesky HA, Rapoport B. Aberrant iodine autoregulation induces hypothyroidism in a mouse strain in the absence of thyroid autoimmunity. *J Endocr Soc* 2018; 2(1):63–76; doi: 10.1210/js.2017-00400
13. Drugarin D, Negru S, Koreck A, et al. The pattern of a TH1 cytokine in autoimmune thyroiditis. *Immunol Lett* 2000; 71(2):73–77; doi: 10.1016/S0165-2478(99)00156-X
14. Nanba T, Watanabe M, Inoue N, et al. Increases of the Th1/Th2 cell ratio in severe Hashimoto's disease and in the proportion of Th17 cells in intractable Graves' disease. *Thyroid* 2009;19(5):495–501; doi: 10.1089/thy.2008.0423
15. Kawakami Y, Kuzuya N, Watanabe T, et al. Induction of experimental thyroiditis in mice by recombinant interferon gamma administration. *Acta Endocrinol (Copenh)* 1990; 122(1):41–48; doi: 10.1530/ACTA.0.1220041
16. Tang H, Mignon-Godefroy K, Meroni PL, et al. The effects of a monoclonal antibody to interferon-gamma on experimental autoimmune thyroiditis (EAT): Prevention of disease and decrease of EAT-specific T cells. *Eur J Immunol* 1993;23(1):275–278; doi: 10.1002/EJI.1830230143
17. Braley-Mullen H, Yu S. Early requirement for B cells for development of spontaneous autoimmune thyroiditis in NOD.H-2h4 mice. *J Immunol* 2000;165(12):7262–7269; doi: 10.4049/jimmunol.165.12.7262
18. Nelms K, Keegan a D, Zamorano J, et al. The IL-4 receptor: Signaling mechanisms and biologic functions. *Annu Rev Immunol* 1999;17:701–738; doi: 10.1146/annurev.immunol.17.1.701
19. Mueller R, Krahl T, Sarvetnick N. Pancreatic expression of interleukin-4 abrogates insulinitis and autoimmune diabetes in nonobese diabetic (NOD) mice. *J Exp Med* 1996;184(3): 1093–1099; doi: 10.1084/jem.184.3.1093
20. Fort MM, Lesley R, Davidson NJ, et al. IL-4 exacerbates disease in a Th1 cell transfer model of colitis. *J Immunol* 2001;166(4):2793–2800; doi: 10.4049/jimmunol.166.4.2793
21. Ramanathan S, de Kozak Y, Saoudi A, et al. Recombinant IL-4 aggravates experimental autoimmune uveoretinitis in rats. *J Immunol* 1996;157(5):2209–2215.
22. Mignon-Godefroy K, Brazillet MP, Rott O, et al. Distinctive modulation by IL-4 and IL-10 of the effector function of murine thyroglobulin-primed cells in "transfer-experimental autoimmune thyroiditis." *Cell Immunol* 1995;162(2):171–177; doi: 10.1006/cimm.1995.1066
23. Tang H, Sharp GC, Peterson KE, et al. Induction of granulomatous experimental autoimmune thyroiditis in IL-4 gene-disrupted mice. *J Immunol* 1998;160:155–162.
24. Yu S, Sharp GC, Braley-Mullen H. Dual roles for IFN-gamma, but not for IL-4, in spontaneous autoimmune thyroiditis in NOD.H-2h4 mice. *J Immunol* 2002;169(7): 3999–4007; doi: 10.4049/jimmunol.169.7.3999
25. Merakchi K, Djerbib S, Soleimani M, et al. Murine thyroid IL-4 expression worsens hypothyroidism on iodine restriction and mitigates Graves disease development. *Endocrinology* 2022;163(9); doi: 10.1210/endo/bqac107
26. Eskalli Z, Achouri Y, Hahn S, et al. Overexpression of IL-4 in the thyroid of transgenic mice upregulates the expression of Duox1 and the anion transporter Pendrin. *Thyroid* 2016; 26(10):1499–1512; doi: 10.1089/thy.2016.0106
27. Podolin PL, Pressey A, DeLarato NH, et al. I-E+ nonobese diabetic mice develop insulinitis and diabetes. *J Exp Med* 1993;178(3):793–803; doi: 10.1084/jem.178.3.793
28. Chen CR, Hamidi S, Braley-Mullen H, et al. Antibodies to thyroid peroxidase arise spontaneously with age in NOD.H-2h4 mice and appear after thyroglobulin antibodies. *Endocrinology* 2010;151(9):4583–4593; doi: 10.1210/en.2010-0321
29. McLachlan SM, Aliesky HA, Rapoport B. To reflect human autoimmune thyroiditis, thyroid peroxidase (not thyroglobulin) antibodies should be measured in female (not sex-independent) NOD. H2h4 mice. *Clin Exp Immunol* 2019; 196(1):52–58; doi: 10.1111/cei.13249
30. Perret J, Ludgate M, Libert F, et al. Stable expression of the human TSH receptor in CHO cells and characterization of differentially expressing clones. *Biochem Biophys Res Commun* 1990;171(3):1044–1050; doi: 10.1016/0006-291X(90)90789-P
31. Bankhead P, Loughrey MB, Fernández JA, et al. QuPath: Open source software for digital pathology image analysis. *Sci Rep* 2017;7(1):1–7; doi: 10.1038/s41598-017-17204-5
32. Pfaffl MW. A new mathematical model for relative quantification in real-time RT-PCR. *Nucleic Acids Res* 2001; 29(9):1–6; doi: 10.1093/nar/29.9.e45
33. Burniat A, Jin L, Detours V, et al. Gene expression in RET/PTC3 and E7 transgenic mouse thyroids: RET/PTC3 but not E7 tumors are partial and transient models of human papillary thyroid cancers. *Endocrinology* 2008;149(10): 5107–5117; doi: 10.1210/en.2008-0531
34. Yu S, Medling B, Yagita H, et al. Characteristics of inflammatory cells in spontaneous autoimmune thyroiditis of NOD.H-2h4 mice. *J Autoimmun* 2001;16(1):37–46; doi: 10.1006/jaut.2000.0458
35. Horie I, Abiru N, Nagayama Y, et al. T helper type 17 immune response plays an indispensable role for development of iodine-induced autoimmune thyroiditis in nonobese diabetic-H2h4 mice. *Endocrinology* 2009;150(11):5135–5142; doi: 10.1210/en.2009-0434
36. Eng PHK, Cardona GR, Fang S-L, et al. Escape from the acute Wolff-Chaikoff effect is associated with a decrease in thyroid sodium/iodide symporter messenger ribonucleic acid and protein 1. *Endocrinology* 1999;140(8):3404–3410; doi: 10.1210/endo.140.8.6893
37. Shen X, Yan X, Xie B, et al. Genetic variants of interleukin-4 gene in autoimmune thyroid diseases: An updated meta-analysis. *Autoimmunity* 2015;48(2):129–135; doi: 10.3109/08916934.2014.962025
38. Nanba T, Watanabe M, Akamizu T, et al. The -590CC genotype in the IL4 gene as a strong predictive factor for the development of hypothyroidism in Hashimoto disease. *Clin Chem* 2008;54(3):621–623; doi: 10.1373/clinchem.2007.099739
39. Racke MK, Bonomo A, Scott DE, et al. Cytokine-induced immune deviation as a therapy for inflammatory autoimmune disease. *J Exp Med* 1994;180(5):1961–1966; doi: 10.1084/jem.180.5.1961
40. Braley-Mullen H, Yu S. NOD.H-2h4 mice: An Important and Underutilized Animal Model of Autoimmune Thyroiditis and Sjogren's Syndrome. *Adv Immunol* 2015;126: 1–43; doi: 10.1016/bs.ai.2014.11.001
41. Barin JG, Afanasyeva M, Talor MV, et al. Thyroid-specific expression of IFN- $\gamma$  limits experimental autoimmune thyroiditis by suppressing lymphocyte activation in cervical lymph nodes. *J Immunol* 2003;170(11):5523–5529; doi: 10.4049/jimmunol.170.11.5523
42. Sharma R, Alegria JD, Talor MV, et al. Iodine and IFN- $\gamma$  synergistically enhance intercellular adhesion molecule 1

- expression on NOD.H2 h4 mouse thyrocytes. *J Immunol* 2005;174(12):7740–7745; doi: 10.4049/jimmunol.174.12.7740
43. Bonita RE, Rose NR, Rasooly L, et al. Adhesion molecules as susceptibility factors in spontaneous autoimmune thyroiditis in the NOD-H2h4 mouse. *Exp Mol Pathol* 2002; 73(3):155–163; doi: 10.1006/exmp.2002.2470
  44. Lee YW, Kühn H, Hennig B, et al. IL-4-induced oxidative stress upregulates VCAM-1 gene expression in human endothelial cells. *J Mol Cell Cardiol* 2001;33(1):83–94; doi: 10.1006/JMCC.2000.1278
  45. Bagnasco M, Pesce GP, Caretto A, et al. Follicular thyroid cells of autoimmune thyroiditis may coexpress ICAM-1 (CD54) and its natural ligand LFA-1 (CD11a/CD18). *J Allergy Clin Immunol* 1995;95(5 Pt 1):1036–1043; doi: 10.1016/s0091-6749(95)70105-2
  46. Striz I, Mio T, Adachi Y, et al. IL-4 induces ICAM-1 expression in human bronchial epithelial cells and potentiates TNF- $\alpha$ . *Am J Physiol Cell Mol Physiol* 1999;277(1):L58–L64; doi: 10.1152/ajplung.1999.277.1.L58
  47. Reinecker HC, Podolsky DK. Human intestinal epithelial cells express functional cytokine receptors sharing the common gamma c chain of the interleukin 2 receptor. *Proc Natl Acad Sci U S A* 1995;92(18):8353–8357; doi: 10.1073/pnas.92.18.8353
  48. Vella V, Mineo R, Frasca F, et al. Interleukin-4 stimulates papillary thyroid cancer cell survival: Implications in patients with thyroid cancer and concomitant Graves' disease. *J Clin Endocrinol Metab* 2004;89(6):2880–2889; doi: 10.1210/jc.2003-031639
  49. Bogusławska J, Godlewska M, Gajda E, et al. Cellular and molecular basis of thyroid autoimmunity. *Eur Thyroid J* 2022;11(1):e210024; doi: 10.1530/ETJ-21-0024
  50. Ludgate M. Animal Models of Autoimmune Thyroid Disease. In: *Autoimmune Diseases in Endocrinology*. (Weetman AP, ed.) Humana Press: Totowa, NJ; 2008; pp. 79–93; doi: 10.1007/978-1-59745-517-6\_4
  51. Martin AP, Coronel EC, Sano G, et al. A novel model for lymphocytic infiltration of the thyroid gland generated by transgenic expression of the CC chemokine CCL21. *J Immunol* 2004;173(8):4791–4798; doi: 10.4049/jimmunol.173.8.4791
  52. Hidaka Y, Okumura M, Shimaoka Y, et al. Increased serum concentration of interleukin-5 in patients with Graves' disease and Hashimoto's thyroiditis. *Thyroid* 1998;8(3): 235–239; doi: 10.1089/thy.1998.8.235
  53. Gopalakrishnan S, Sen S, Adhikari JS, et al. The role of T-lymphocyte subsets and interleukin-5 blood levels among Indian subjects with autoimmune thyroid disease. *Hormones (Athens)* 2010;9(1):76–81; doi: 10.14310/horm.2002.1256
  54. Ajjan RA, Weetman AP. Cytokines in thyroid autoimmunity. *Autoimmunity* 2003;36(6–7):351–359; doi: 10.1080/08916930310001603046
  55. Leung AM, Braverman LE. Iodine-induced thyroid dysfunction. *Curr Opin Endocrinol Diabetes Obes* 2012;19(5): 414–419; doi: 10.1097/MED.0B013E3283565BB2

Address correspondence to:

*Xavier De Deken, PhD*

*DUOX Lab*

*Faculté de Médecine*

*Institut de Recherche Interdisciplinaire en Biologie*

*Humaine et Moléculaire (IRIBHM)*

*Université libre de Bruxelles (ULB)*

*Campus Erasme, Bat C. Local C4-147*

*808, Route de Lennik*

*1070 Bruxelles*

*Belgium*

*E-mail: xavier.de.deken@ulb.be*